The Fundamental Property of Human Leg During Walking: Linearity and Nonlinearity

Kunyang Wang, *Member, IEEE*, Amaraporn Boonpratatong, Wei Chen, Lei Ren, *Member, IEEE*, Guowu Wei, *Member, IEEE*, Zhihui Qian, Xuewei Lu, and Di Zhao

***Abstract*— Leg properties have been involved in the broad study of human walking from mechanical energy to motion prediction of robotics. However, the variable leg elasticities and their functions during gait have not been fully explored. This study presented that the fundamental leg properties during human walking comprise axial stiffness, rest leg length, tangential stiffness and force-free leg angles. We measured the axial force-leg length and tangential force-leg angle data in eight participants (mean ± s.d. age 24.6 ± 3.0 years, mass 68.2 ± 6.8 kg, height 177.5 ± 5.2 cm) at three self-selected walking speeds (slow: 1.25 ± 0.22, normal: 1.48 ± 0.28, fast: 1.75 ± 0.32 m/s) on two different contact conditions (fixed and moving). After obtaining these gait measurements, we extracted the linear and nonlinear leg elasticities during human walking by using a minimum root-mean-square fitting. We found that the axial stiffness of nonlinear elasticity (fixed condition: 7.1−8.0, moving condition: 21.3−22.6) is higher than that of the linear elasticity (fixed condition: 5.0−5.7, moving condition: 15.2−16.5). The tangential stiffness behaves different during four stance phases of gait, with the highest (linear: 2.52−3.72, nonlinear: 1.71−2.01, in moving condition) occurred at early stance and second highest at late stance, followed by two stiffnesses in mid-stance. For both linearity and nonlinearity, the axial stiffness and rest length are independent of walking speeds in both contact conditions, while the tangential stiffness and contact angles are independent of walking speeds only in moving condition. Regardless of walking speed, elasticity and contact condition, the force-free contact angle at mid-stance is maintained at average of 82.2°. This paper first demonstrates the mechanical walking leg property from both axial and tangential aspects. The findings provide insight into the fundamental properties including linearity and nonlinearity of human leg during locomotion for stability analysis and precise motion prediction of robotics and rehabilitation exoskeletons.**

***Index Terms*— Rehabilitation, leg elasticity, human walking, linearity, nonlinearity, leg stiffness, biomechanics.**

I. Introduction

WALKING is the most fundamental and widespread form of transportation for human being. The complex functions of the human leg during locomotion may be briefly categorised into three classes: energy conservation, power attenuation and power amplification [1]. The combination of these functions performs sophisticated locomotion that a human does in daily-life with high efficiency and low energy consumption. This may be a consequence of the design of structural organisms in the legs and other body parts, which was adapted from generation to generation for certain functions [2], [3], [4]. Leg properties has involved in the broad study of human walking ranging from basic mechanical work to the motion prediction of robotics and rehabilitation exoskeletons by using spring-mass model [5], [6]. In the study of basic mechanical work, the leg elasticity plays a crucial role in the mechanical energy changes during the gait cycle [7], [8], [9]. In human locomotion prediction, the spring stiffness is a crucial elastic leg property transforming the change in leg length to that in leg force and vice versa. This basic leg property aims to address the global elasticity of the whole-body structure as a consequence of joint elasticity [10], [11], [12].

Compliant legged machines operated on the conservation of system energy have been found to inherit the self-stability [5], [13], [14], [15], [16], [17], [18]. In a certain energy range, the well-tuned combinations of linear elastic leg properties and touchdown timing defined by leg angle and leg length at touchdown instant are required to carry out periodic motion of walking and running. It was found that the orbital stability of the gait decays with higher leg stiffness [13], [15], [16]. Most studies of leg stiffness during human locomotion have been based on the change in leg length and the total ground reaction

Manuscript received 28 September 2023; revised 25 November 2023; accepted 3 December 2023. Date of publication 5 December 2023; date of current version 13 December 2023. This work was supported in part by the National Natural Science Foundation of China under Grant 52005209, Grant 91948302, Grant 91848204, Grant 52021003; and in part by the Natural Science Foundation of Jilin Province under Grant 20210101053JC. *(Corresponding authors: Lei Ren; Xuewei Lu.)*

This work involved human subjects or animals in its research. Approval of all ethical and experimental procedures and protocols was granted by the Human Research Ethics Committee at The Second Hospital of Jilin University under Application No. 2020085.

Kunyang Wang, Lei Ren, and Xuewei Lu are with the Key Laboratory of Bionic Engineering, Ministry of Education, Jilin University, Changchun 130025, China, and also with the School of Mechanical, Aerospace and Civil Engineering, University of Manchester, M13 9PL Manchester, U.K. (e-mail: lren@jlu.edu.cn; xwlu@jlu.edu.cn).

Amaraporn Boonpratatong is with the School of Mechanical, Aerospace and Civil Engineering, University of Manchester, M13 9PL Manchester, U.K.

Wei Chen, Zhihui Qian, and Di Zhao are with the Key Laboratory of Bionic Engineering, Ministry of Education, Jilin University, Changchun 130025, China.

Guowu Wei is with the School of Science, Engineering and Environment, University of Salford, M5 4WT Salford, U.K.

Digital Object Identifier 10.1109/TNSRE.2023.3339801

force (GRF) considered to apply along the leg axis [19], [20], [21], [22], [23], [24], [25]. For instance, a linear axial force-leg deflection relationship was used to extract the elastic property and angle of attack of the leg [23]. The dimensionless leg stiffness of 29–45 and 21–23 and the attack angle ranging from 68–85 and 73–88 degrees were found during human walking and running, respectively.

However, the total ground reaction force during the gait does not always apply along the leg axis. In the joint level, when the human body is considered as a multi-segment system, it has been found that the coordination of joint elasticity and the geometry of multi-segment body during locomotion results in the centre of mass motion in parallel and perpendicular direction to the leg axis [10], [11], [26]. Thus, the projection of the resultant force onto both directions needs to be addressed carefully to account for all corresponding mechanical properties of the human leg during locomotion. The rotational elasticity in human walking has been studied by using spring-mass model with hip joint and torso [27]. This model addresses the relationship between the components of total ground reaction force, the axial and rotational elasticity during human walking. Although, the predicted ground reaction force and hip torque profile are slightly different from that in human walking experiments, the relationship between ground reaction force components and the axial and rotational elasticity were found to be very important in human walking stabilisation [27].

Most of the study of leg properties during the human locomotion primarily focused on linear elasticity, until it has been found recently that the changes in leg stiffness and rest length during the gait improve the human running prediction of the spring-loaded-inverted pendulum (SLIP) model [28], [29]. The improved running prediction resulted from variable leg properties supports the previous findings that the nonlinear elasticity can stabilise the spring leg robot after perturbation and touchdown impact. The soft nonlinear elasticity was found to stabilise the spring leg running after perturbation better than linear elasticity [30], while the hard nonlinear elasticity was found to stabilise the gait pattern after touchdown impact [31]. The variation of leg stiffness during the gait is likely another mechanical property facilitating in negotiation with small perturbation. Leg positioning, i.e. leg angle at touchdown and take-off, has been found as one of the crucial adjustments for the contact duration and phase transition in biped locomotion [32], [33], [34]. Predicted by the spring-mass model, the change of touchdown angle with the change in leg stiffness was found to regulate the energy transfers during the gait cycle [15], [16], [19], [32], [35]. However, such adjustment during human locomotion has not been fully investigated.

In brief, the leg properties, primarily including the elastic properties and the leg positioning have been found as crucial mechanical properties of the human leg during locomotion. The proper combination of the axial and rotational or tangential stiffness, rest length and the leg positioning are required to predict the precise walking motion and phase transition. Depending on available human walking measurements and purpose of study, these leg properties during the walking motion can be estimated by different leg property definitions. However, the variable leg properties during human gait have not been fully explored possibly due to the experimental limitations and complexity of musculoskeletal structure. The coordination between axial and rotational actuation found to enhance perturbation resistance in biped robot simulation has never been investigated in human locomotion.

Therefore, an overall objective of our study was to provide insight into the fundamental leg properties including linearity and nonlinearity factors during locomotion, which could facilitate the stability analysis and precise motion prediction of robotics and lower-limb rehabilitation devices. Anticipations of the fundamental leg elasticities can provide stability analysis and precise prediction of human or robotic locomotion [5], [6], [36]. We hypothesised that the minimal leg properties that will be essential to identify human leg mechanics during walking not only exhibit linear and nonlinear elasticities, but also axial and tangential stiffnesses, and they are possibly independent from walking speeds. To address our hypotheses, we measured the single valued force-displacement relationships during walking at three self-selected speeds and extracted the basic mechanical properties of human leg by using a minimum root-mean-square fitting. Actual and normalised values of axial stiffness, rest leg length, tangential stiffness and force-free leg angles were quantified in both fixed and moving contact conditions.

II. Materials and Methods

A. Experimental Protocol

Eight healthy male adults with no previous medical history of bone or joint injury (mean ± s.d. age 24.6 ± 3.0 years, mass 68.2 ± 6.8 kg, height 177.5 ± 5.2 cm) participated in this study. All participants provided informed consent before participating in the protocol, which was approved by the Human Research Ethics Committee at The Second Hospital of Jilin University (No. 2020085). They were asked to walk on the walkway under three different self-selected speeds: slow (1.25 ± 0.22 m/s), normal (1.48 ± 0.28 m/s) and fast (1.75 ± 0.32 m/s). Each walking speed was measured 10 times. Kinematic data was collected at 200 Hz using an eight-infrared camera motion capture system (Qualisys, Sweden), and ground reaction force/moment data were recorded at 1000 Hz by using a six-force plate array (Kistler, Switzerland).

For each subject, the movement of 13 major body segments (the head, torso, pelvis, right and left humerus, right and left forearms, and both legs comprising thighs, shanks and feet) were recorded. A group of specially designed thermoplastic plates, each carrying a cluster of four reflective markers, were attached to each body segment [37]. A head band was used to carry the four markers on the head. An elastic hip belt was used to firmly locate the plastic plate carrying the four markers on the pelvis. Plastic plates and the helmet reduce the relative movement between the markers on a segment, thereby improving the accuracy of the measured data [38].

In total, 52 reflective markers were used to capture whole-body motion during the walking trials. In order to decrease the effect of relative motions between the reflective markers and bones, anatomical landmarks determined from

the positions of the reflective markers were used to define the local coordinate system of each segment. The anatomical landmarks were located from a series of static calibration procedures by using a calibration wand and reflective markers. A wand with two reflective markers was used to determine the spatial positions of the anatomical landmarks on pelvis which were not conveniently defined by reflective markers. The calibration markers were then removed before walking tests according to the calibrated anatomical system technique [39]. Other anatomical landmarks were determined directly using reflective markers. With the local coordinate system of each segment, the whole-body motion was obtained by rigid multi-body dynamics. The functional approach [40], [41] was used to determine the hip joint centre. Other joint centres were defined based on anatomical landmarks.

B. Data Processing

For data analysis, we discarded the trials with more than 10 consecutive missing frames. The raw data of all successful trials were processed using a custom MATLAB based package, GMAS (General Motion Analysis Software) [37], which has been developed for 3D kinematic and kinetic analysis of general biomechanical multibody systems. After fill-gap processing, the data were filtered using a low pass zero lag fourth-order Butterworth digital filter with a cut-off frequency of 6.0 Hz. The segment positions and orientations were defined in an anatomically significant way. From the static calibration data, the relative positions of the anatomical landmarks with respect to the technical markers were obtained. For some anatomical landmarks i.e. shoulders and hips, the reconstruction based on dynamic calibration trials (functional method) was used. As the joint centre positions were described in local coordinate system of the adjacent segment, the transformation from local to global coordinate system was employed. Thereafter, given the derived anatomical landmark position, the poses of the anatomical coordinate systems were obtained for each sampled instant of time.

Given the poses of the anatomical coordinate systems, the location of segment mass centre was determined from the relevant anatomical landmarks, where some three-dimensional anthropometric data was used [42]. The linear velocities and accelerations of the segment mass centre were then calculated using the finite difference methods [43]. For the ground reaction forces and moments, the transformation matrix from the force plate local coordinate system to the global reference coordinate system was derived and then used to transform the ground reaction forces and moments to the global reference frame. The location of the centre of pressure (CoP) was then determined by the application point of the ground reaction force in global reference frame.

C. Calculation of Leg Motion and CoM Trajectory

Gait cycles are marked by two events (touchdown and take-off) of the same foot. The touchdown (td) is defined as the instant when the foot-ground contact initially occurs without exerted force. In the measurement, the GRF is initially detected when it is above zero. The numerical extrapolation [43] was applied to the GRF records to estimate the instance and CoP location at the zero GRF. Accordingly, the take-off (to) is defined as the final instant of the foot-ground contact when the GRF reduces to zero. A similar numerical extrapolation technique is used to estimate the instant and CoP location for the take-off (to). The leg length and leg angle were then calculated between the touchdown and take-off of the same leg. The centres of mass motion of major body segments at each sampled instant of time were calculated by the GMAS software. The position and velocity of the whole-body centre of mass in three-dimensional space can be calculated by rigid multibody dynamics. First, the position of the whole-body CoM at touchdown instant is defined as the summation of the mass of each body segment multiplying the CoM position of each corresponding body segment dividing the whole-body mass. Subsequently, the velocity of the whole-body CoM at touchdown instant was calculated by deriving the whole-body CoM position. Then, based on Newton's Second Law, the position and velocity of the whole-body CoM at touchdown was used as initial condition to derive the whole-body CoM motion (position and velocity) at the subsequent instance by integrating ground reaction forces during given time instances.

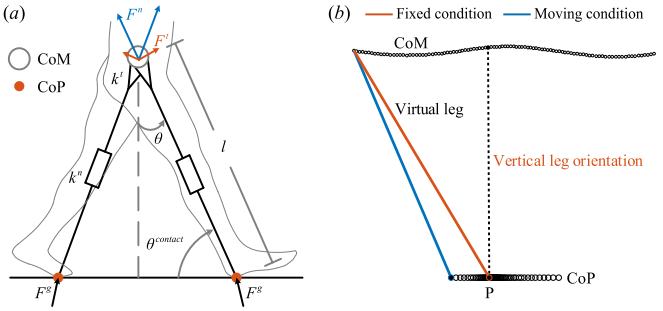

Fig. 1. Schematic illustration of human walking. (a) The mechanical system of human walking. It is represented by leg length l, leg angle θ, contact angle $\theta^{contact}$, axial stiffness k^n and tangential stiffness k^t, axial force F^n and tangential force F^t (as the projections of the total ground reaction force F^g). (b) Two contact conditions between the foot and the ground. The virtual leg in moving contact condition (blue) is defined by a straight line connecting between the centre of mass (CoM) and the moving contact. The moving contact is defined by the location of the centre of pressure (CoP). The virtual leg in fixed contact condition (red) is defined by a straight line connecting between the CoM and the fixed contact. The fixed contact P is defined by the CoP at which the virtual leg on moving contact reaches the vertical leg orientation (dash).

D. Axial Stiffness and Rest Length

Fundamental leg properties comprising leg stiffness, rest leg length and three force-free leg angles are proposed to express leg elasticity and phase transition, which are necessary mechanical properties to representation the human walking. In this study, the fundamentals of mechanical properties of the human leg are defined and extracted from the measurement data by a technique of minimum root-mean-squares error (RMSE) fitting. The virtual leg is defined as a straight leg represented by a line connecting the centre of mass (CoM) and the foot-ground contact point (Fig. 1a). The foot-ground contact point is defined in two conditions (Fig. 1b). The first condition considers the moving contact calculated from the anterior-posterior position of the centre of pressure (CoP) for each foot. The second condition considers the fixed contact P

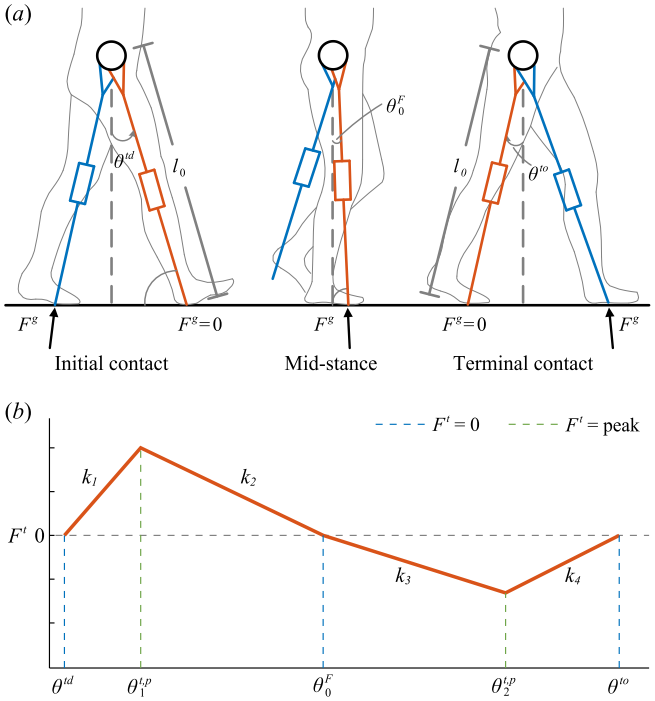

Fig. 2. Definitions of leg properties. (a) Force-free leg length and leg angles. Force-free leg length l_0 occurs at initial and terminal contact when the ground reaction force (GRF) F^g is zero, and force-free leg angle θ_0 occurs at initial contact $\theta_0 = \theta^{td}$, mid-stance $\theta_0 = \theta_0^F$ and terminal contact $\theta_0 = \theta^{to}$ when the tangential leg force is zero. Red line is stance leg, and blue line is swing leg. (b) Tangential leg properties. They comprises four of tangential stiffness (k_1, k_2, k_3, k_4), three of force-free leg angles (θ^{td}, θ_0^F, θ^{to}◁ and leg angles at first and second force peaks ($\theta_1^{t,p}$, $\theta_2^{t,p}$).

defined by the CoP where the virtual leg on moving contact reaches vertical leg orientation.

The leg stiffness comprises axial and tangential stiffnesses. The axial stiffness is derived from the leg compression-extension, the rest leg length and the projection of the total ground reaction force onto the virtual leg so called axial force. The axial stiffness (k^n) and rest length (l_0) will be extracted from the axial force-leg length relationship on both linear and nonlinear elasticity of the virtual leg. For the linear elasticity, the axial force-leg length relationship is defined as

$$F_{lin}^n = k_{lin}^n(l_0 - l) \tag{1}$$

where F_{lin}^n is the projection of the total ground reaction force onto the virtual leg axis, l is the virtual leg length, k_{lin}^n is the linear axial stiffness and l_0 is the rest length which is the force-free leg length at initial and terminal contact. The force-free leg length (l_0) is the leg length when the ground reaction force is zero during the ground contact (see Fig. 2a).

To represent the nonlinear elasticity, the axial force-leg length relationship is defined as

$$\begin{aligned} F_{nln}^n &= k_{nln}^n(l_0 - l) \\ k_{nln}^n &= k_{lin,b}^n(1 + a \cdot e^b(l_0 - l)) \end{aligned} \tag{2}$$

where k_{nln}^n is the nonlinear stiffness as a quadratic function of leg deflection $(l_0 - l)$, $k_{lin,b}^n$ is basic linear stiffness, a is a coefficient of nonlinear stiffness, b is exponential power of nonlinear coefficient. The square of axial deflection $(l_0 - l)$ expresses the moderate strength of nonlinearity. This exponential-quadratic form requires only two parameters to fit the axial-force leg length relationship. The preliminary examination on other nonlinear forms such as Fourier series, pure exponential and pure quadratic functions showed that more parameters are required while the RMSE is not significantly reduced.

E. Tangential Stiffness and Force-Free Leg Angles

The tangential stiffness is derived from the angular deflection of the virtual leg and the projection of the total ground reaction force onto the perpendicular line of the virtual leg. The leg angle is defined as the angle between the virtual leg and the vertical. The angle made by virtual leg and the horizontal is defined as contact angle.

The tangential stiffness (k^t) and force-free leg angle (θ_0) will be extracted from the relationships between tangential force and leg angle. Both linear and nonlinear elasticity will be examined. The tangential force-leg angle relationship for linear elasticity is defined as:

$$\begin{aligned} F_{lin}^t &= \frac{k_{lin}^t}{l}(\theta_0 - \theta) \\ k_{lin}^t &= \begin{cases} -k_1 & \text{if } \theta^{td} \le \theta \le \theta_1^{t,p} \\ k_2 & \text{if } \theta_1^{t,p} \le \theta \le \theta_0^F \\ k_3 & \text{if } \theta_0^F \le \theta \le \theta_2^{t,p} \\ -k_4 & \text{if } \theta_2^{t,p} \le \theta \le \theta^{to} \end{cases} \\ \theta_0 &= \begin{cases} \theta^{td} & \text{if } \theta^{td} \le \theta \le \theta_1^{t,p} \\ \theta_0^F & \text{if } \theta_1^{t,p} \le \theta \le \theta_2^{t,p} \\ \theta^{to} & \text{if } \theta_2^{t,p} \le \theta \le \theta^{to} \end{cases} \end{aligned} \tag{3}$$

where F_{lin}^t is the projection of the total ground reaction force onto the perpendicular line of the virtual leg, θ is the leg angle, l is the virtual leg length, k_{lin}^t is the linear tangential stiffness, θ^{td} and θ^{to} are the leg angle at touchdown (td) and take-off (to), respectively, θ_0^F is the leg angle when the total ground reaction force applies through the leg axis (i.e. tangential force becomes zero), $\theta_1^{t,p}$ and $\theta_2^{t,p}$ are the leg angles at the first and second peak of the tangential force, respectively. θ_0 is the rest angle or the force-free leg angle at initial contact (td), mid-stance and terminal contact (to) when the tangential force is zero. The illustrations of tangential leg properties are shown in Fig. 2b. The force-free leg angles were assumed to change discretely according to the change of tangential force.

For the nonlinear elasticity, the tangential force-leg angle relationship is defined by

$$\begin{aligned} F_{nln}^t &= \left(\sum_{n=1}^{2}(a_n(\cos\frac{n\pi\theta^*}{p} - 1) + b_n \sin\frac{n\pi\theta^*}{p})\right)/l \\ \theta^* &= \theta - \theta^{td} \\ p &= \frac{\theta^{to} - \theta^{td}}{2} \end{aligned} \tag{4}$$

where a_n and b_n are the Fourier coefficients for the fluctuation of tangential force. The Fourier series were selected from the nonlinear functions including exponential and polynomial function that can give minimum RMSE by using

minimum number of parameters. The preliminary examination on Fourier series in higher order showed that the RMSE is not significantly reduced.

In order to compare between the linear and nonlinear elasticity, the stiffness on maximum force and displacement so called total stiffness (z) [2] is used, which can be given by

$$z^n = \frac{(max(F^n) - min(F^n))}{(l_{min} - l_0)}$$
$$z^t = \frac{(max(F^t) - min(F^t))}{(\theta_{min} - \theta_0)} \quad (5)$$

for the axial stiffness (z^n) and for the tangential stiffness (z^t).

F. Leg Property Extraction

To estimate the axial stiffness (k^n) and the rest length (l_0), the minimisation of root-mean-square error is used to fit the force equations onto the axial force-leg length data sets obtained from the walking measurement. For each subject, the data set of the virtual leg length and the leg force for all the three trials is fed into (1) to estimate the linear axial stiffness (k^n) and the rest length (l_0) that minimises the difference between the measured force and calculated force quantified by RMSE. The minimization of the RMSE is operated by using optimisation function "fmincon" in MATLAB (MathWorks, Natick, MA, USA). With the similar scheme, (2) is used to estimate the nonlinear axial stiffness (k^n) and the corresponding rest length (l_0).

The linear tangential stiffness (k^t) and force-free leg angle (θ_0) are estimated by feeding the data set of the leg angle and the leg length into (3) and following the similar optimisation scheme. For the nonlinear elasticity of the tangential force, the Fourier coefficients (a_m, b_m), the leg angle at touchdown (θ^{td}) and take-off (θ^{to}) are estimated by feeding the measurement data of the leg angle and the leg length into (4). After the equation parameters were determined by the minimum RMSE fitting, the force equations are substituted into (5) to calculate the total stiffness or mechanical impedance (z) for axial and tangential stiffness, respectively. The total stiffness (z) is used to compare the linear and nonlinear elasticity. This extraction procedure is different from those in other studies in which the linear least squares method was used to find the axial stiffness and rest length that minimise the square error regardless the violation of perfect elasticity [23], [44]. Overall, the axial force-leg length and tangential force-leg angle relationships in fixed and moving contact conditions are calculated from measurement data of the CoM, CoP and ground reaction force at three walking speeds for each subject. The leg properties for linear and nonlinear elasticity of the virtual leg are then extracted.

G. Statistical Analysis

A priori power analysis was first conducted to determine the sample size using SPSS 25.0 software (IBM, USA). A sample size of eight subjects is adequate to evaluate ANOVA for repeated measures (within–between interactions), achieving statistical power greater than 0.80 at 0.25 effect size and 0.05 probability level (P value). Another statistical analysis was then performed to evaluate whether axial stiffness, rest leg length, tangential stiffness and force-free leg angles change with different speeds from slow to fast walk using SPSS 25.0 software (IBM, USA). For each condition, mean ± s.d. were calculated across all subjects and trials. They were then analysed separately by using the analysis of variance (ANOVA) with repeated measurements based on a linear mixed model approach considering intra- and inter-subject variability (random effects: subjects and trials; fixed effects: walking speed). The statistical significance level of all tests was set to $p = 0.05$, and all data is presented at $p < 0.05$ unless otherwise stated.

TABLE I
GENERAL INFORMATION OF INDIVIDUAL SUBJECT

Subject	Age (yeas old)	Weight (kg)	Height (cm)	l^{st} (mm)
No. 1	26	67.2	177.1	895.2
No. 2	24	69.3	179.2	913.9
No. 3	31	53.5	165.3	839.8
No. 4	25	71.2	181.4	917.6
No. 5	22	79.0	180.7	931.7
No. 6	21	65.5	178.1	926.2
No. 7	22	72.1	182.9	919.1
No. 8	26	68.0	175.1	896.2

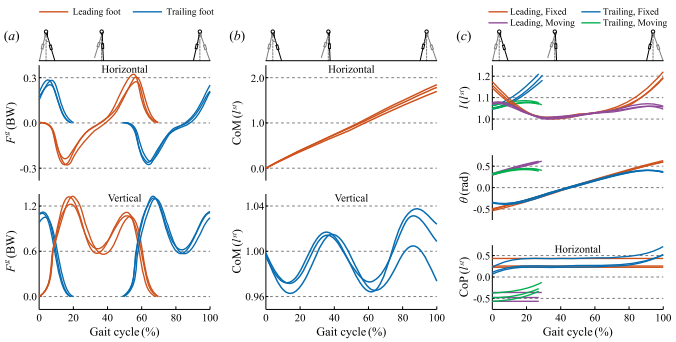

Fig. 3. Representative of the 3D whole-body walking measurements. Shown are normalised ground reaction forces on the leading and trailing feet (a), normalised whole-body CoM trajectories (b), and leg lengths, leg angles and CoP for leading and trailing legs in fixed and moving conditions (c) during a gait. The dataset was obtained from three representative trials of the walking measurements of one subject (No. 2) at normal walking speed. CoM, centre of mass; CoP, centre of pressure. BW, body weight; l^{st}, leg length at still standing.

III. RESULTS

Eight healthy male subjects participated in this study and their information were listed in Table I. The key measurements of one subject (No. 2) were depicted in Fig. 3, including the 3D motion data of ground reaction forces (Fig. 3a), the calculated whole-body CoM motion in sagittal plane (Fig. 3b), the leg lengths, leg angles and CoP calculated in the fixed and moving contact conditions (Fig. 3c). These data were combined to investigate the axial and tangential leg properties during human walking.

A. Linear Axial Stiffness and Rest Length

Fig. 4a and 4b show the relationship of axial force and rest length, as well as their linear fits, during human walking at fixed and moving contact conditions. For all walking speeds

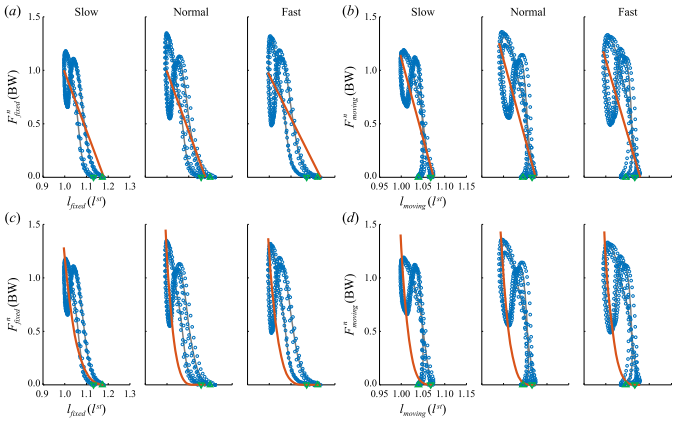

Fig. 4. The linear and nonlinear fits of axial leg force as well as rest length during walking. (a) and (c) show normalised axial force F^n, normalised leg length l, and their linear (a) and nonlinear (c) fits at fixed contact condition. (b) and (d) show these measured and fitting data at moving contact condition. The dataset (blue circles) was obtained from three representative trials of the walking measurements of one subject (No. 2) at all three walking speeds (slow, normal, fast). The linear and nonlinear fits (red lines) were conducted by the minimum root-mean-square error (RMSE) fitting. BW, body weight; l^{st}, leg length at still standing; ∇, touchdown (td); $\scriptstyle 1$, take-off (to).

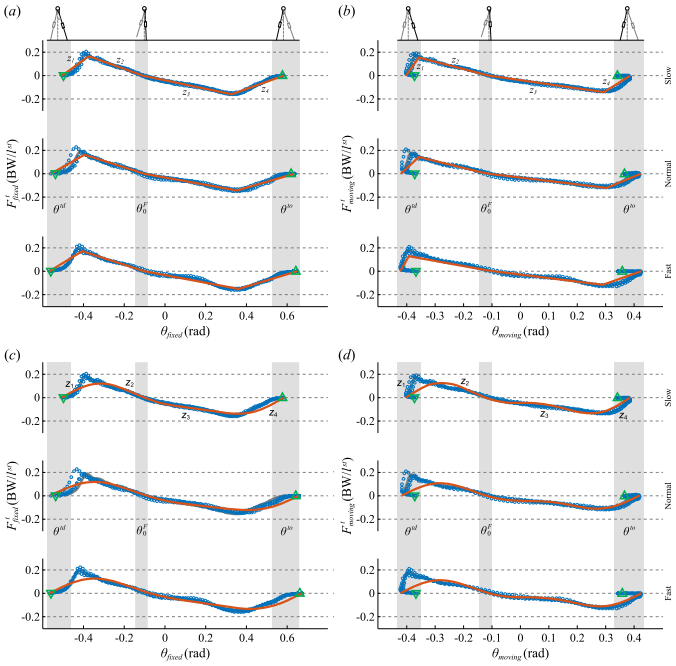

Fig. 5. The linear and nonlinear fits of tangential leg force as well as leg angle during walking. (a) and (c) show the normalised tangential force F^t, leg angle θ, and their linear (a) and nonlinear (c) fits at fixed contact condition. (b) and (d) show these measured and fitting data at moving contact condition. The dataset (blue circles) was obtained from three representative trials of the walking measurements of one subject (No. 2) at all three walking speeds (slow, normal, fast). The linear and nonlinear fits (red lines) were conducted by the minimum root-mean-square error (RMSE) fitting. Shaded are three force-free leg angles (θ^{td}, θ_0^F, θ^{to}). BW, body weight; l^{st}, leg length at still standing; ∇, touchdown (td); Δ, take-off (to).

in the fixed condition, the measured leg length at touchdown is shorter than that at take-off, the measured leg length at maximum shortening is close to that during still standing (l^{st}), and the linear elastic fitting underestimates the axial force at maximum leg shortening. In the moving condition, the measured leg length at touchdown is longer than that at take-off. Similar to the fixed contact condition, the measured leg length at maximum shortening is close to that during still standing (l^{st}). Compared with the linear elastic leg properties on fixed contact at the same speed, the linear elastic leg properties on moving contact have shorter rest length (l_0) and higher total axial stiffness (z^n_{lin}).

B. Nonlinear Axial Stiffness and Rest Length

Fig. 4c and 4d show the relationship of axial force and rest length, as well as their nonlinear fits, during human walking at fixed and moving contact conditions. It appears that the nonlinear elastic fitting overestimates the fixed contact axial force around maximum leg shortening for slow and normal walking. Compared with the linear elastic leg properties on the same contact condition at same walking speed, the nonlinear elastic leg properties have higher total axial stiffness (z^n_{nln}) and generally shorter rest length (l_0). For all walking speeds, the nonlinear elastic fitting overestimates the moving contact axial force when the leg is at the maximum leg shortening. Compared to the linear elastic leg properties in the same contact condition at the same walking speed, the nonlinear elastic leg properties have higher total axial stiffness (z^n_{nln}) and nearly the same rest length (l_0). In addition, compared to the nonlinear elastic leg properties in fixed contact condition at same walking speed, the nonlinear elastic leg properties in moving contact condition have higher total axial stiffness (z^n_{nln}) and shorter rest length (l_0).

C. Linear Tangential Stiffness and Force-Free Leg Angles

Fig. 5a and 5b illustrate the relationship of tangential force and leg angle, as well as their linear fits, during human walking at fixed and moving contact conditions. The results show that in the fixed contact condition at all walking speeds, the absolute value of force-free leg angle at touchdown (θ^{td}) is smaller than that at take-off (θ^{to}). The total tangential stiffness (z^t_{lin}) is highest at the early stance. The force-free leg angle at mid stance (θ_0^F) hardly changes with walking speed. In moving contact condition, the absolute value of force-free leg angles at touchdown (θ^{td}) and take-off (θ^{to}) at each walking speed are nearly equivalent. Similar to that in fixed contact condition, the total tangential stiffness (z^t_{lin}) is highest at the early stance for all walking speeds. For linear elasticity, the total tangential stiffness (z^t_{lin}) in moving contact condition is higher than that in fixed contact condition at the same speed.

D. Nonlinear Tangential Stiffness and Force-Free Leg Angles

Fig. 5c and 5d illustrate the relationship of tangential force and leg angle, as well as their linear fits, during human walking at fixed and moving contact conditions. It appears that in fixed contact condition for all walking speeds, the nonlinear elastic

TABLE II
AXIAL AND TANGENTIAL LEG PROPERTIES DURING HUMAN WALKING

				Slow		Normal		Fast	
				moving CoP	fixed CoP	moving CoP	fixed CoP	moving CoP	fixed CoP
Axial leg properties									
total dynamic stiffness (z^n)	linear	actual (kN m)		12.0 ± 2.5	4.2 ± 0.8	11.0 ± 1.7	3.6 ± 0.9	11.2 ± 2.5	4.0 ± 1.3
		normalised		16.5 ± 2.0	5.7 ± 0.6	15.2 ± 1.8	5.0 ± 0.7	15.3 ± 2.2	5.4 ± 1.2
	nonlinear	actual (kN m)		16.6 ± 4.1	5.8 ± 0.8	15.5 ± 3.5	5.2 ± 0.8	16.0 ± 3.5	5.6 ± 0.7
		normalised		22.6 ± 3.9	8.0 ± 0.6	21.3 ± 3.5	7.1 ± 0.9	22.0 ± 3.1	7.7 ± 0.5
rest length (l_0)	linear	actual (m)		0.960 ± 0.034	1.043 ± 0.033	0.962 ± 0.040	1.076 ± 0.041	0.964 ± 0.038	1.075 ± 0.049
		normalised		1.062 ± 0.017	1.155 ± 0.033	1.064 ± 0.018	1.191 ± 0.033	1.066 ± 0.017	1.189 ± 0.043
	nonlinear	actual (m)		0.957 ± 0.030	1.045 ± 0.026	0.960 ± 0.037	1.048 ± 0.022	0.963 ± 0.034	1.045 ± 0.017
		normalised		1.059 ± 0.018	1.157 ± 0.026	1.062 ± 0.018	1.161 ± 0.041	1.065 ± 0.016	1.157 ± 0.039
Tangential leg properties									
total dynamic stiffness (z^t)	linear	actual (kN m rad^{-1})	k_1	2.18 ± 0.70	0.76 ± 0.19	1.68 ± 0.48	0.73 ± 0.29	2.50 ± 0.81	0.68 ± 0.15
			k_2	0.39 ± 0.06	0.34 ± 0.13	0.33 ± 0.07	0.29 ± 0.07	0.29 ± 0.05	0.17 ± 0.31
			k_3	0.21 ± 0.05	0.24 ± 0.06	0.20 ± 0.04	0.22 ± 0.04	0.20 ± 0.04	0.12 ± 0.20
			k_4	0.93 ± 0.33	0.46 ± 0.13	0.85 ± 0.21	0.40 ± 0.06	0.90 ± 0.35	0.40 ± 0.08
		normalised	k_1	3.24 ± 0.74	1.17 ± 0.19	2.52 ± 0.43	1.12 ± 0.30	3.72 ± 0.94	0.96 ± 0.15
			k_2	0.59 ± 0.04	0.52 ± 0.13	0.49 ± 0.06	0.44 ± 0.07	0.44 ± 0.05	0.26 ± 0.31
			k_3	0.32 ± 0.04	0.36 ± 0.06	0.30 ± 0.05	0.34 ± 0.04	0.31 ± 0.03	0.19 ± 0.20
			k_4	1.38 ± 0.40	0.71 ± 0.13	1.32 ± 0.40	0.63 ± 0.06	1.39 ± 0.55	0.54 ± 0.08
	nonlinear	actual (kN m rad^{-1})	k_1	1.26 ± 0.12	0.57 ± 0.08	1.37 ± 0.14	0.55 ± 0.09	1.35 ± 0.20	0.50 ± 0.10
			k_2	0.29 ± 0.03	0.23 ± 0.08	0.35 ± 0.12	0.25 ± 0.07	0.30 ± 0.07	0.26 ± 0.08
			k_3	0.20 ± 0.05	0.21 ± 0.05	0.22 ± 0.04	0.20 ± 0.03	0.23 ± 0.14	0.21 ± 0.05
			k_4	0.52 ± 0.16	0.44 ± 0.10	0.59 ± 0.12	0.37 ± 0.06	0.62 ± 0.18	0.41 ± 0.10
		normalised	k_1	1.71 ± 0.12	0.91 ± 0.10	2.01 ± 0.16	0.89 ± 0.12	1.86 ± 0.25	0.82 ± 0.14
			k_2	0.40 ± 0.03	0.32 ± 0.10	0.49 ± 0.14	0.35 ± 0.08	0.43 ± 0.10	0.36 ± 0.10
			k_3	0.27 ± 0.05	0.29 ± 0.06	0.30 ± 0.04	0.27 ± 0.04	0.31 ± 0.19	0.29 ± 0.05
			k_4	0.70 ± 0.17	0.60 ± 0.13	0.82 ± 0.13	0.52 ± 0.08	0.85 ± 0.20	0.56 ± 0.11
contact angle ($\theta^{contact}$) or 90°+θ	linear	θ^{td} (deg)		66.5 ± 1.1	60.8 ± 0.8	66.0 ± 0.5	58.9 ± 0.8	65.6 ± 1.0	57.8 ± 0.5
		θ_1^{tp} (deg)		69.1 ± 0.9	66.9 ± 0.9	68.8 ± 0.6	65.7 ± 0.9	67.6 ± 1.0	64.7 ± 1.2
		θ_0^{F} (deg)		82.2 ± 2.3	82.3 ± 1.4	82.6 ± 1.4	82.3 ± 1.9	83.9 ± 1.9	81.8 ± 1.8
		θ_2^{tp} (deg)		-73.1 ± 0.2	-70.6 ± 2.0	-71.9 ± 1.5	-68.9 ± 1.0	-72.3 ± 1.3	-68.7 ± 1.3
		θ^{to} (deg)		-66.7 ± 2.3	-56.2 ± 2.4	-65.8 ± 0.8	-53.3 ± 1.5	-65.7 ± 0.9	-53.4 ± 1.3
	nonlinear	θ^{td} (deg)		66.2 ± 1.3	60.8 ± 0.7	65.8 ± 0.4	59.0 ± 0.7	65.1 ± 1.1	57.9 ± 0.6
		θ_1^{tp} (deg)		78.2 ± 0.7	70.0 ± 1.1	72.6 ± 0.6	69.1 ± 0.8	72.3 ± 1.1	68.0 ± 1.4
		θ_0^{F} (deg)		79.8 ± 1.6	82.9 ± 1.6	81.1 ± 1.6	82.6 ± 1.6	82.4 ± 1.5	82.2 ± 2.1
		θ_2^{tp} (deg)		-75.4 ± 1.2	-69.8 ± 1.6	-74.3 ± 0.6	-68.3 ± 1.2	-74.2 ± 0.3	-67.3 ± 0.9
		θ^{to} (deg)		-66.0 ± 2.2	-56.2 ± 2.3	-65.3 ± 0.8	-53.3 ± 1.6	-65.2 ± 0.9	-53.4 ± 1.2

Data are means ± s.d. for all the participants and all the trials. The total axial stiffness (z^n) is normalised by body weight (BW) and leg length during still standing (l^{st}). The rest length is normalised by leg length during still standing (l^{st}). θ^{td}, θ_0^F, θ^{to} are the force-free leg angles at touchdown, mid-stance, take-off, respectively, and θ_1^{tp}, θ_2^{tp} are the leg angles at the first and second peak of the tangential force, respectively.

fitting underestimates the first peak of tangential force. In the same contact condition and at the same walking speed, total tangential stiffness (z^t_{nln}) of the nonlinear elasticity is lower than that of linear elasticity. In moving contact condition at all walking speeds, the nonlinear elastic fitting underestimate the first peak of tangential force. In the same contact condition and at the same walking speed, the total tangential stiffness (z^t_{nln}) of nonlinear elasticity is lower than that of linear elasticity. However, this total tangential stiffness (z^t_{nln}) of nonlinear elasticity in moving contact condition is higher than that in fixed contact condition.

E. Comparison Between the Linear and Nonlinear Leg Stiffness

The actual and normalised values of the axial and tangential leg properties for all three walking speeds and all the participants are processed for both fixed and moving contact condition. Table II shows the axial properties comprising total axial stiffness (z^n) and rest length (l_0) during walking, as well as the tangential properties comprising total tangential stiffness (z^t) and contact angle ($\theta^{contact}$) at slow, normal and fast speed. The total stiffness (z^n) is normalised by body weight (BW) and leg length during still standing (l^{st}). The rest length is normalised by leg length during still standing (l^{st}). The contact angle is the angle between the virtual leg and horizontal or $\theta^{contact} = 90° + \theta$ as shown in Fig. 1. It comprises five different angles (θ^{td}, $\theta F0$, θ^{to}, $\theta t,p1$, $\theta t,p2$) to address the changes in magnitude and direction of the tangential leg force during the contact (Fig. 3b). Due to the smaller leg deflection ($l_0 - l$), the axial stiffness in the moving contact condition (linear: 11.0−12.0 kN m, nonlinear: 15.5−16.6 kN m) is higher than that in fixed contact condition (linear: 3.6−4.2 kN m, nonlinear: 5.2−5.8 kN) as seen in Fig. 4. The axial dynamic stiffness of nonlinear elasticity (dimensionless of 7.1−8.0 in fixed condition and 21.3−22.6 in moving condition) is higher than that of the linear elasticity (dimensionless of 5.0−5.7 in fixed condition and 15.2−16.5 in moving condition) in both

contact conditions at all walking speeds. From both elasticity fittings in both contact conditions, the total axial stiffness (z^n) and rest length (l_0) are independent of walking speeds.

The total tangential stiffness (z^t) change according to the changes in magnitude and direction of the tangential force during the gait (Fig. 5). The overall trend of four stiffness (k_1, k_2, k_3, k_4) during different phases of gait is similar, which has the highest k_1 and second highest k_4, followed by k_2 and k_3. This total tangential stiffness (z^t) in fixed contact condition (linear: 0.12−0.76 kN m rad^{-1}, nonlinear: 0.20−0.57 kN m rad^{-1}) is lower than that in moving contact condition (linear: 0.20−2.50 kN m rad^{-1}, nonlinear: 0.20−1.37 kN m rad^{-1}). Similarly, the absolute value of contact angle at touchdown and take-off (53.3°−60.8° for both linear and nonlinear) in fixed contact condition is smaller than that in moving contact condition (linear: 65.7°−66.5°, nonlinear: 65.2°−66.2°). The total stiffness of the nonlinear elasticity (dimensionless of 0.27−0.91 in fixed condition and 0.27−2.01 in moving condition) is lower than that of linear elasticity (dimensionless of 0.19−1.17 in fixed condition and 0.30−3.72 in moving condition) because the nonlinear elastic fitting using second-order Fourier series in (4) cannot capture the peak tangential force.

In fixed contact condition, for both linear and nonlinear elasticity, the tangential stiffness and the absolute value of contact angle at touchdown and take-off decrease as the walking speed increases. However, in moving contact condition, the tangential stiffness and the absolute value of those contact angles are independent of the walking speed. Regardless of the walking speed, elasticity fitting and contact condition, the force-free contact angle at mid-stance (θ_0^F) is maintained at average of 82.2° with respect to the ground.

IV. Discussion

In this study, the fundamentals of mechanical properties of human leg during walking have been proposed, which represent the minimal leg properties that are necessary to identify human leg mechanics during walking motion. The axial and tangential properties were extracted from the axial force-leg length and tangential force-leg angle relationships on the virtual leg during human walking. The effects of walking speed and foot-ground contact condition were investigated.

The combination of the extracted linear axial stiffness (k_{lin}^n) and touchdown contact angle (θ^{td}) on the moving contact condition falls within the stable range of the leg parameters in the compliant leg model with axial elastic property developed by Geyer et al. [15]. Their compliant leg model with axial elastic property was operated by axial leg force alone, which predicted that the axial stiffness is dependent on walking speed. Although, the changes of axial stiffness and contact angle in Table II are speed-independent, it falls within the parameter range of the compliant leg model [15], which can reproduce the stable walking motion at speed 1.0−1.5 m/s.

The speed independence of the linear axial properties in our study is consistent with that in the literature [23]; however, their normalised axial stiffness and contact angle are much higher. We found the axial stiffness from 21.3 to 22.6 at walking speed from 1.25 to 1.78 m/s. In their study, the total ground reaction force obtained from the walking and running measurement was considered to apply along the virtual leg. Such scheme provides the normalised axial stiffness between 31.7 to 45.8 for speed between 1.04 to 2.07 m/s. The periodic walking simulation was found only with the axial stiffness being 33.1 and contact angle being 74.8° at walking speed of 1.04 m/s. On the same leg property definition, Lipfert et al. [23] also presented higher axial stiffness during running than that calculated by Coleman et al. [44] which used similar force projection technique as our study to extract axial stiffness from human running measurement. For the nonlinear axial properties, the speed independence is also found. Only the hard nonlinear elasticity can achieve the minimum RMSE fits on the axial force-leg length data. Compared with the linear elastic fittings in the fixed contact condition, the nonlinear elastic fittings better fit the axial force-leg length data in early and middle stance; however, it overestimates the axial force when the leg is at the maximum leg shortening.

There are no previous studies on the tangential leg properties from the walking measurement extraction. Only the hip torque profile during the gait cycle has been introduced by Maus et al. [27]. Such torque profile to stabilise the human upright walking agrees with our tangential force-leg angle relationship in Fig. 5. The tangential stiffness behaves different during four phases of gait, with the highest k_1 (linear: 2.52−3.72 in moving condition and 0.96−1.17 in fixed condition, nonlinear: 1.71−2.01 in moving condition and 0.82−0.91 in fixed condition) at early stance and second highest k_4 (linear: 1.32−1.39 in moving condition and 0.54−0.71 in fixed condition, nonlinear: 0.70−0.85 in moving condition and 0.52−0.60 in fixed condition) at late stance, followed by k_2 and k_3 (linear: 0.30−0.59 in moving condition and 0.19−0.52 in fixed condition, nonlinear: 0.27−0.49 in moving condition and 0.27−0.36 in fixed condition) in mid-stance. The speed dependence is found in the tangential properties for both linear and nonlinear elasticity on the fixed contact condition. However, the nonlinear fittings by using second order Fourier series on the tangential force-leg angle data underestimate the tangential stiffness in early and late stance.

On the effects of foot-ground contact condition, the higher axial and tangential stiffness of the moving contact condition than that of the fixed contact condition are consistent with previous studies [45], [46]. For both linearity and nonlinearity, the axis stiffness in moving condition is approximately three times as high as that in fixed condition at all three speeds. In comparison, the tangential stiffness in moving condition is approximately twice the value in fixed condition at all three speeds. As the foot-ground contact moves forward during the stance, the shortening-lengthening ($l_0 - l$) and angular deflection ($\theta_0 - \theta$) of the virtual leg are reduced and thus, increase the total axial and tangential stiffness.

The effects of linear and nonlinear elasticity, foot-ground contact condition and ground reaction force decomposition underline the influence of leg property definition on the extracted leg properties. In fact, there is only a short period during the mid-stance that the direction of total ground reaction force coincides with the leg axis. By projecting the total ground reaction force onto the parallel and perpendicular line

of the virtual leg, the axial and tangential stiffness can be estimated from the more realistic force-displacement relationships. Compared to the linear elasticity, the nonlinear elasticity better fits on the axial force-leg length relationship of fixed contact condition. The different foot-ground contact conditions result in distinct force-displacement patterns, leading to different leg properties extracted based on leg definitions. The implementation of these mechanical leg properties in human walking model is required to validate the leg property region in human walking prediction.

In addition to the fitting, other calculations may also affect the leg properties extraction. One of which is the calculation for centre of mass motion. In our study, the centre of mass motion at the touchdown instant during walking is used as the initial motion to integrate the ground reaction force. Other studies prevented the signal drifts by starting the integration from the still standing [21], [23]. However, to study human walking at self-selected speed, the latter technique requires a long walking track or a measurement conducted on treadmill. It has been found that the variation of CoM velocity during the over-ground and treadmill walking are fundamentally different [18], [47], [48], [49], [50]. This may lead to different estimations of CoM motion and thus different force-displacement relationships. Extracted from walking measurements on treadmill, Lipfert et al. [23] found that the rest length is shorter than the leg length at still standing. Such leg properties limit the implementation in compliant leg model with axial elastic property and thus some adjustments were required to validate those leg properties with human walking measurements. In addition, human legs were simplified as straight lines which made it more convenient to calculate fundamental leg parameters including rest leg length, axial and tangential stiffness, and force-free leg angles. However, legs are not always straight especially during late stance phase. The bending motion would affect the calculations of the leg forces, which might cause the deviation of research conclusions.

The speed independence of the extracted mechanical leg properties can be interpreted in many different ways. It may imply that the leg elasticity during human walking does not change with walking speed. More implication may be from the fitting function. The single valued force-displacement relationships used in all fittings has some limitations to extract the mechanical leg properties during human walking. The measured axial force-leg length relationships in both contact conditions are non-conservative around the maximum leg shortening (Fig. 4). By fitting the single valued force-length function onto such non-conservative relationship, the rest length is stretched to the maximum length to satisfy the spring leg equation (Fig. 4) and may affect the extracted axial stiffness shown in (1) and (2). Similarly, for the tangential properties on the moving contact condition, single valued force-angle function overestimates the absolute leg angle at touchdown and take-off (Fig. 5). It may affect the extracted tangential stiffness shown in (3). In such cases, the parametric equations may be required to express the multi-valued force-angle and force-length functions for the extraction of axial and tangential leg properties from the force-displacement relationships during human walking.

A bipedal walking model based on the proposed elastic leg properties could be used to predict the human walking motion of robotics and lower-limb exoskeletons by using the minimal inputs of axial leg properties and initial contact angle (θ^{td}). In a particular range of walking motion, the proper combinations of axial leg stiffness (k^n) and touchdown leg angle (θ^{td}) are required to produce periodic walking motion. However, this production is rather sensitive to the initial condition of the walking motion especially the initial forward speed (v_0) which regulates the forward rotation of CoM with respect to the contact point. The proper horizontal speed allows sufficient duration for the upright CoM, which allows the proper energy transfer among potential, strain and kinetic energy. As a result, the proper oscillation of the CoM on the compliant leg is created, which regulates the initiation and termination of double support phase and forward progression the CoM to complete the walking step. In this model, the CoM oscillation increases with increased walking speed. The CoM becomes airborne and fails to complete walking cycle when the walking speed exceeds 1.5 m/s [15]. This walking speed limit of the compliant leg walking template restricts the human walking prediction based on the axial elastic leg properties to the moderate walking speed. Depending on the axial leg properties alone, the CoM motion predicted by compliant leg walking model is regulated by the touchdown contact angle (θ^{td}), axial stiffness (k^n) and the initial condition of the CoM motion. The incorporation of the tangential component of the leg force or the rotational elasticity of the virtual leg may render to extend the walking speed range predicted by the leg walking model for controlling robots and exoskeletons.

V. Conclusion

Leg properties has involved in the broad study of human walking from mechanical energy to motion prediction of robotics. This paper first demonstrates the linear and nonlinear mechanical walking leg property from both axial and tangential aspects. The axial force-leg length and tangential force-leg angle data at slow, normal and fast walking speeds were measured to extract the axial and tangential stiffnesses at two contact conditions by linear and nonlinear fittings. The rest leg length and force-free leg angles during walking were also included as the key parameters. The findings provide insight into the fundamental properties including linearity and nonlinearity of human leg during locomotion for stability analysis and precise motion prediction of robotics and rehabilitation exoskeletons.

Symbols and Abbreviations

a	Coefficient of nonlinear stiffness.
a_m, b_m	Fourier coefficients.
a_n, b_n	Fourier coefficients for the fluctuation of tangential force.
b	Exponential power of nonlinear coefficient.
BW	Body weight.
CoP	Centre of pressure.

CoM	Centre of mass.
F^g	Total ground reaction force.
F^n	Axial force, i.e., projection of the total ground reaction force onto the virtual leg axis.
F^t	Tangential force, i.e., projection of the total ground reaction force onto the perpendicular line of the virtual leg.
F^n_{lin}	Linear axial force.
F^t_{lin}	Linear tangential force.
F^n_{nln}	Nonlinear axial force.
F^t_{nln}	Nonlinear tangential force.
F^n_{fixed}	Fixed contact axial force.
F^t_{fixed}	Fixed contact tangential leg force.
F^n_{moving}	Moving contact axial force.
F^t_{moving}	Moving contact tangential leg force.
GRF	Ground reaction force.
k^n	Axial stiffness.
k^t	Tangential stiffness.
k^n_{lin}	Linear axial stiffness.
k^t_{lin}	Linear tangential stiffness.
k^n_{nln}	Nonlinear axial stiffness.
$k^n_{lin,b}$	Basic linear stiffness.
k_1, k_2, k_3, k_4,	Tangential leg properties comprising four of tangential stiffness.
l	Virtual leg length.
l^{st}	Leg length obtained during still standing.
l_{fixed}	Fixed contact leg length.
l_{moving}	Moving contact leg length.
l_0	Rest length.
RMSE	Root-mean-square error.
z	Total stiffness or mechanical impedance.
z^n	Total axial stiffness.
z^t	Total tangential stiffness.
z^n_{lin}	Total linear axial stiffness.
z^t_{lin}	Total linear tangential stiffness.
z^n_{nln}	Total nonlinear axial stiffness.
z^t_{nln}	Total nonlinear tangential stiffness.
θ	Leg angle.
$\theta^{contact}$	Contact angle.
θ^{td}	Leg angle at touchdown.
θ^{to}	Leg angle at take-off.
θ_0	Force-free leg angle.
θ^F_0	Leg angle when the total ground reaction force applies through the leg axis (tangential leg force is zero).
$\theta^{t,p}_1$	Leg angle at the first peak in the tangential force.
$\theta^{t,p}_2$	Leg angle at the second peak in the tangential force.
θ_{fixed}	Fixed contact leg angle.
θ_{moving}	Moving contact leg angle.
∇	Touchdown.
Δ	Take-off.

REFERENCES

[1] T. J. Roberts and E. Azizi, "Flexible mechanisms: The diverse roles of biological springs in vertebrate movement," *J. Experim. Biol.*, vol. 214, no. 3, pp. 353–361, Feb. 2011, doi: 10.1242/jeb.038588.

[2] S. A. Wainwright, W. D. Biggs, J. D. Currey, and J. M. Gosline, *Mechanical Design in Organisms*. London, U.K.: Edward Arnold, 1976.

[3] J. M. DeSilva et al., "The lower limb and mechanics of walking in australopithecus *sediba*," *Science*, vol. 340, no. 6129, Apr. 2013, Art. no. 1232999, doi: 10.1126/science.1232999.

[4] N. B. Holowka and D. E. Lieberman, "Rethinking the evolution of the human foot: Insights from experimental research," *J. Experim. Biol.*, vol. 221, no. 17, Sep. 2018, Art. no. 174425, doi: 10.1242/jeb.174425.

[5] R. Blickhan, A. Seyfarth, H. Geyer, S. Grimmer, H. Wagner, and M. Günther, "Intelligence by mechanics," *Phil. Trans. Roy. Soc. A, Math., Phys. Eng. Sci.*, vol. 365, no. 1850, pp. 199–220, Jan. 2007, doi: 10.1098/rsta.2006.1911.

[6] M. Srinivasan and A. Ruina, "Computer optimization of a minimal biped model discovers walking and running," *Nature*, vol. 439, no. 7072, pp. 72–75, Jan. 2006, doi: 10.1038/nature04113.

[7] G. A. Cavagna, H. Thys, and A. Zamboni, "The sources of external work in level walking and running," *J. Physiol.*, vol. 262, no. 3, pp. 639–657, Nov. 1976, doi: 10.1113/jphysiol.1976.sp011613.

[8] G. A. Cavagna, N. C. Heglund, and C. R. Taylor, "Mechanical work in terrestrial locomotion: Two basic mechanisms for minimizing energy expenditure," *Amer. J. Physiol.-Regulatory, Integrative Comparative Physiol.*, vol. 233, no. 5, pp. R243–R261, Nov. 1977, doi: 10.1152/ajpregu.1977.233.5.r243.

[9] F. L. Haufe, P. Wolf, R. Riener, and M. Grimmer, "Biomechanical effects of passive hip springs during walking," *J. Biomech.*, vol. 98, Jan. 2020, Art. no. 109432, doi: 10.1016/j.jbiomech.2019.109432.

[10] R. M. Alexander, "The spring in your step: The role of elastic mechanisms in human running," in *Biomechanics XI-A* (International Series on Biomechnaics), G. de Groot, G. Hollander, A. Huijing, and P. van Ingen Schenau, Eds. Amsterdam, The Netherlands: Free Univ. Press, 1988, pp. 17–25.

[11] M. H. Pope, "Elastic mechanisms in animal movement," *J. Biomech.*, vol. 23, no. 1, p. 103, Jan. 1990, doi: 10.1016/0021-9290(90)90375-D.

[12] A. M. Selvitella and K. L. Foster, "The spring-mass model and other reductionist models of bipedal locomotion on inclines," *Integrative Comparative Biol.*, vol. 62, no. 5, pp. 1320–1334, Dec. 2022, doi: 10.1093/icb/icac047.

[13] J. Rummel, Y. Blum, H. M. Maus, C. Rode, and A. Seyfarth, "Stable and robust walking with compliant legs," in *Proc. IEEE Int. Conf. Robot. Autom.*, May 2010, pp. 5250–5255, doi: 10.1109/ROBOT.2010.5509500.

[14] A. Seyfarth et al., "Running and walking with compliant legs," in *Fast Motions in Biomechanics and Robotics*. Berlin, Germany: Springer, 2006, pp. 383–401.

[15] H. Geyer, A. Seyfarth, and R. Blickhan, "Compliant leg behaviour explains basic dynamics of walking and running," *Proc. Roy. Soc. B, Biol. Sci.*, vol. 273, no. 1603, pp. 2861–2867, Nov. 2006, doi: 10.1098/rspb.2006.3637.

[16] H. Geyer, A. Seyfarth, and R. Blickhan, "Spring-mass running: Simple approximate solution and application to gait stability," *J. Theor. Biol.*, vol. 232, no. 3, pp. 315–328, Feb. 2005, doi: 10.1016/j.jtbi.2004.08.015.

[17] A. Seyfarth, H. Geyer, M. Günther, and R. Blickhan, "A movement criterion for running," *J. Biomech.*, vol. 35, no. 5, pp. 649–655, May 2002, doi: 10.1016/S0021-9290(01)00245-7.

[18] N. Seethapathi and M. Srinivasan, "Step-to-step variations in human running reveal how humans run without falling," *eLife*, vol. 8, Mar. 2019, Art. no. e38371, doi: 10.7554/elife.38371.

[19] T. A. Mcmahon and G. C. Cheng, "The mechanics of running: How does stiffness couple with speed?" *J. Biomech.*, vol. 23, pp. 65–78, Jan. 1990, doi: 10.1016/0021-9290(90)90042-2.

[20] C. R. Lee and C. T. Farley, "Determinants of the center of mass trajectory in human walking and running," *J. Experim. Biol.*, vol. 201, no. 21, pp. 2935–2944, Nov. 1998, doi: 10.1242/jeb.201.21.2935.

[21] Y. Blum, S. W. Lipfert, and A. Seyfarth, "Effective leg stiffness in running," *J. Biomech.*, vol. 42, no. 14, pp. 2400–2405, Oct. 2009, doi: 10.1016/j.jbiomech.2009.06.040.

[22] J.-B. Morin, P. Samozino, and G. Y. Millet, "Changes in running kinematics, kinetics, and spring-mass behavior over a 24-h run," *Med. Sci. Sports Exerc.*, vol. 43, no. 5, pp. 829–836, May 2011, doi: 10.1249/mss.0b013e3181fec518.

[23] S. W. Lipfert, M. Günther, D. Renjewski, S. Grimmer, and A. Seyfarth, "A model-experiment comparison of system dynamics for human walking and running," *J. Theor. Biol.*, vol. 292, pp. 11–17, Jan. 2012, doi: 10.1016/j.jtbi.2011.09.021.

[24] T. Ma et al., "Gait phase subdivision and leg stiffness estimation during stair climbing," *IEEE Trans. Neural Syst. Rehabil. Eng.*, vol. 30, pp. 860–868, 2022, doi: 10.1109/TNSRE.2022.3163130.

[25] A. S. Voloshina and D. P. Ferris, "Biomechanics and energetics of running on uneven terrain," *J. Experim. Biol.*, vol. 218, no. 5, pp. 711–719, Mar. 2015, doi: 10.1242/jeb.106518.

[26] M. Günther and R. Blickhan, "Joint stiffness of the ankle and the knee in running," *J. Biomech.*, vol. 35, no. 11, pp. 1459–1474, Nov. 2002, doi: 10.1016/s0021-9290(02)00183-5.

[27] H.-M. Maus, S. W. Lipfert, M. Gross, J. Rummel, and A. Seyfarth, "Upright human gait did not provide a major mechanical challenge for our ancestors," *Nature Commun.*, vol. 1, no. 1, p. 70, Sep. 2010, doi: 10.1038/ncomms1073.

[28] D. M. Dudek and R. J. Full, "Passive mechanical properties of legs from running insects," *J. Experim. Biol.*, vol. 209, no. 8, pp. 1502–1515, Apr. 2006, doi: 10.1242/jeb.02146.

[29] G. T. Burns, R. Gonzalez, and R. F. Zernicke, "Improving spring-mass parameter estimation in running using nonlinear regression methods," *J. Experim. Biol.*, vol. 224, no. 6, Mar. 2021, Art. no. 242787, doi: 10.1242/jeb.232850.

[30] J. D. Karssen and M. Wisse, "Running with improved disturbance rejection by using non-linear leg springs," *Int. J. Robot. Res.*, vol. 30, no. 13, pp. 1585–1595, Nov. 2011, doi: 10.1177/0278364911408631.

[31] D. Owaki and A. Ishiguro, "Enhancing self-stability of a passive dynamic runner by exploiting nonlinearity in the leg elasticity," in *Proc. SICE-ICASE Int. Joint Conf.*, Nov. 2006, pp. 4532–4537, doi: 10.1109/SICE.2006.315037.

[32] C. T. Farley and O. González, "Leg stiffness and stride frequency in human running," *J. Biomech.*, vol. 29, no. 2, pp. 181–186, Feb. 1996, doi: 10.1016/0021-9290(95)00029-1.

[33] M. A. Daley and A. A. Biewener, "Running over rough terrain reveals limb control for intrinsic stability," *Proc. Nat. Acad. Sci. USA*, vol. 103, no. 42, pp. 15681–15686, Oct. 2006, doi: 10.1073/pnas.0601473103.

[34] R. Müller, A. V. Birn-Jeffery, and Y. Blum, "Human and avian running on uneven ground: A model-based comparison," *J. Roy. Soc. Interface*, vol. 13, no. 122, Sep. 2016, Art. no. 20160529, doi: 10.1098/rsif.2016.0529.

[35] J. P. Folland, S. J. Allen, M. I. Black, J. C. Handsaker, and S. E. Forrester, "Running technique is an important component of running economy and performance," *Med. Sci. Sports Exerc.*, vol. 49, no. 7, pp. 1412–1423, Jul. 2017, doi: 10.1249/mss.0000000000001245.

[36] S. J. Hasaneini, J. E. A. Bertram, and C. J. B. Macnab, "Energy-optimal relative timing of stance-leg push-off and swing-leg retraction in walking," *Robotica*, vol. 35, no. 3, pp. 654–686, Mar. 2017, doi: 10.1017/s0263574715000764.

[37] L. Ren, R. K. Jones, and D. Howard, "Dynamic analysis of load carriage biomechanics during level walking," *J. Biomech.*, vol. 38, no. 4, pp. 853–863, Apr. 2005, doi: 10.1016/j.jbiomech.2004.04.030.

[38] E. H. Garling et al., "Soft-tissue artefact assessment during step-up using fluoroscopy and skin-mounted markers," *J. Biomech.*, vol. 40, pp. S18–S24, Jan. 2007, doi: 10.1016/j.jbiomech.2007.03.003.

[39] A. Cappozzo, F. Catani, U. D. Croce, and A. Leardini, "Position and orientation in space of bones during movement: Anatomical frame definition and determination," *Clin. Biomech.*, vol. 10, no. 4, pp. 171–178, 1995, doi: 10.1016/0268-0033(95)91394-T.

[40] A. Cappozzo, "Gait analysis methodology," *Hum. Mov. Sci.*, vol. 3, nos. 1–2, pp. 27–50, Mar. 1984, doi: 10.1016/0167-9457(84)90004-6.

[41] S. S. H. U. Gamage and J. Lasenby, "New least squares solutions for estimating the average centre of rotation and the axis of rotation," *J. Biomech.*, vol. 35, no. 1, pp. 87–93, Jan. 2002, doi: 10.1016/s0021-9290(01)00160-9.

[42] P. de Leva, "Adjustments to Zatsiorsky–Seluyanov's segment inertia parameters," *J. Biomech.*, vol. 29, no. 9, pp. 1223–1230, Sep. 1996, doi: 10.1016/0021-9290(95)00178-6.

[43] C. R. Hibbeler, *Engineering Mechanics: Dynamics*, 12th ed. Upper Saddle River, NJ, USA: Prentice-Hall, 2010.

[44] D. R. Coleman, D. Cannavan, S. Horne, and A. J. Blazevich, "Leg stiffness in human running: Comparison of estimates derived from previously published models to direct kinematic-kinetic measures," *J. Biomech.*, vol. 45, no. 11, pp. 1987–1991, Jul. 2012, doi: 10.1016/j.jbiomech.2012.05.010.

[45] B. R. Whittington and D. G. Thelen, "A simple mass-spring model with roller feet can induce the ground reactions observed in human walking," *J. Biomech. Eng.*, vol. 131, no. 1, Jan. 2009, Art. no. 011013, doi: 10.1115/1.3005147.

[46] S. R. Bullimore and J. F. Burn, "Consequences of forward translation of the point of force application for the mechanics of running," *J. Theor. Biol.*, vol. 238, no. 1, pp. 211–219, Jan. 2006, doi: 10.1016/j.jtbi.2005.05.011.

[47] M. Schablowski and H. J. Gerner, "Comparison of two measures of dynamic stability during treadmill walking," in *Fast Motions in Biomechanics and Robotics*. Berlin, Germany: Springer, 2006, pp. 345–360.

[48] F. Dierick, M. Penta, D. Renaut, and C. Detrembleur, "A force measuring treadmill in clinical gait analysis," *Gait Posture*, vol. 20, no. 3, pp. 299–303, Dec. 2004, doi: 10.1016/j.gaitpost.2003.11.001.

[49] J. B. Dingwell, J. P. Cusumano, P. R. Cavanagh, and D. Sternad, "Local dynamic stability versus kinematic variability of continuous overground and treadmill walking," *J. Biomech. Eng.*, vol. 123, no. 1, pp. 27–32, Feb. 2001, doi: 10.1115/1.1336798.

[50] S. C. White, H. J. Yack, C. A. Tucker, and H.-Y. Lin, "Comparison of vertical ground reaction forces during overground and treadmill walking," *Med. Sci. Sports Exerc.*, vol. 30, no. 10, pp. 1537–1542, Oct. 1998, doi: 10.1097/00005768-199810000-00011.